Fredenhagen et al. Journal of Analytical Science and Technology (2017) 8:10
DOI 10.1186/s40543-017-0120-2

Journal of Analytical Science and Technology

RESEARCH ARTICLE Open Access

Human UDP-glucuronosyltransferase UGT1A4 forms tertiary *N*-glucuronides predominately with the energetically less favored tautomer of substituted 1*H*-indazole (benzpyrazole)

Andreas Fredenhagen*, Fabian K. Eggimann, Matthias Kittelmann, Thomas Lochmann and Jürgen Kühnöl

Abstract

Background: Human UDP-glucuronosyltransferase UGT1A4 is reported to convert a range of tertiary amine substrates to the respective quaternary glucuronides. In this study, we report on the in vitro glucuronidation of a substituted 1*H*-indazole (benzpyrazole), a transient receptor potential ankyrin 1 antagonist.

Methods: Depending on the mammalian liver used for production, two peaks with different UV spectra and slightly different MS/MS spectra were found in the LC-MS/MS analysis. An optimized HPLC method gave a baseline separation of the two glucuronides. Preparation and isolation allowed to assign their structure by ^{1}H-, ^{13}C-, and ^{15}N-NMR.

Results: Both nitrogens of this structure were accessible to glucuronidation resulting in the respective tertiary glucuronides. As expected, the *N*-glucuronidation proceeded with marked species difference. Surprisingly, the glucuronide produced by human liver homogenate and by the majority of liver preparations from 11 animal species was attached at the energetically less favorable 2-position, indicating the regioselectivity of the respective enzyme. Among 13 recombinant human UDP-glucuronosyltransferases tested only the isoenzyme 1A4 showed significant formation of both glucuronides with the energetically less favorable *N*-glucuronide in 33-fold excess. An MS/MS fragmentation mechanism was proposed for a fragment loss of 134 Da that differentiated the spectra of the two glucuronides.

Conclusions: This investigation shows that assumptions on the structure of metabolites based on stability of tautomers may be wrong. A novel meachanism to form tertiary N-glucuronides was proposed.

Background

Transient receptor potential (TRP) cation channels are a large family of ion channels of which currently 28 mammalian proteins are known. They are activated by physical stimuli like chemicals, mechanical force and hotness or coldness (Wu et al. 2010). The attractiveness of these cation channels as targets for medicines has increased in the last years. For example, in the year 2011, there were nine compounds with ongoing or terminated clinical studies for pain with antagonists of the TRP vanilloid 1 receptor (Moran et al. 2011). TRP ankyrin 1 (TRPA1) received its name due to a high number of *N*-terminal ankyrin repeats. The receptor contributes to pain sensations by structurally diverse exogenous and endogenous chemicals, whereas its activation by noxious cold is still debated (Wu et al. 2010). Mutations in TRPA1 cause the familial episodic pain syndrome (FEPS) (Kremeyer et al. 2010). Families with this very rare hereditary disease suffer from debilitating upper body pain starting in infancy. These findings and experiments with TRPA1 knockout mice suggest that this receptor is an

* Correspondence: andreas.fredenhagen@novartis.com
Novartis Institutes for BioMedical Research, Global Discovery Chemistry, CH-4002 Basel, Switzerland

attractive drug discovery target to reduce pain (Chen et al. 2012; Koivisto et al. 2014).

In a joint medicinal chemistry program of our colleagues in the Horsham research center (U.K.) and from the Genomics Institute of the Novartis Research Foundation, San Diego, several TRPA1 antagonists for the treatment of pain were identified with IC_{50} values as low as 15 nM (Rooney et al. 2014). Early in vitro metabolism studies with rat or human hepatocytes suggested that the main human metabolite of a promising compound was a glucuronide. This result made it desirable to have sufficient amounts of this glucuronide in hands. In the present study, the screening for the most suitable biocatalyst for glucuronide synthesis, the production of the two found glucuronides, the unambiguous elucidation of their structures, and the responsible human UDP-glucuronosyltransferase for this biotransformation will be presented.

Methods

General

Magnesium chloride powder (208337), uridine 5′-diphosphoglucuronic acid trisodium salt (UDPGA; U6751), adenosine 5′-triphosphate disodium salt hydrate (ATP; A7699), 4-(2-hydroxyethyl)piperazine-1-ethanesulfonic acid (HEPES; H3375), and the Bradford reagent (B6916) were purchased from Sigma-Aldrich. Human liver S9 fraction was from Life Technologies Corp. (Grand Island, NY, USA). Microsomes (supersomes™) of SF9 insect cells (*Spodoptera frugiperda*) having expressed recombinant human (rh) uridine 5′-diphospho-glucuronosyltransferase isoforms (UGTs) as well as liver S9 preparations from rat (male Sprague–Dawley) were purchased from Corning B.V. (Amsterdam, The Netherlands). Animal liver S9 fractions were prepared as described before (Kittelmann et al. 2003). Compound 1 was obtained from Novartis Pharmaceuticals Corporation, and the synthesis has been described (Rooney et al. 2014).

The analytical liquid chromatograph consisted of a Waters UPLC Acquity (Waters, Milford, USA) equipped with a Waters Acquity PDA detector. Column, Acquity BEH C18, 1.7 μm; 1.0 × 150 mm (Waters); flow rate 0.075 ml/min; eluent A, 5 mM ammonium acetate in H_2O/methanol (*v*/*v*; 95:5); eluent B, methanol; gradient, 0 min 10% B; 1 min 40% B; 16 min 70% B; 17–18 min 95% B; column temperature 45 °C; UV detection 240 nm, DAD from 210–350 nm, resolution 2.4 nm; injection volume 0.6 μl. The UPLC was controlled by Empower software (Version 2 or 3). The UV spectra are baseline-corrected.

An ion trap mass spectrometer LTQ Velos Pro (Thermo Scientific, San Jose, CA, USA) equipped with heated electrospray interface was operated in the positive mode with Xcalibur software version 2.1 as follows: A sheath gas (nitrogen, >99.5%) setting of 24 units and auxiliary gas of 5 units was used and a spray voltage of 3.5 kV applied. The heated metal capillary was maintained at 275 °C with a mass range of 250 to 500 Da. The system was optimized for *m/z* 549 $[M + H]^+$ of antimycin A_1 in the positive ion mode. Typical parameters: S-Lens 62%; multipole 00 offset −1.8 V; multipole 0 offset −7.5 V; front lens −9.1 V. MS/MS parameters: CID with isolation width 2.8 Da and without wide-band excitation activated; normalized collision energy 35%; activation time 10 ms.

For accurate mass measurements, a Q Exactive plus (Thermo Scientific) equipped with electrospray interface was operated in the positive mode at high resolution mode (30,000). For preparative purification, a HPLC system Spot Liquid Chromatography Flash, 250 bar (Armen instruments/Dichrome GmbH, Marl, Germany), was used.

Analytical scale glucuronidation

In an 1.5 ml Eppendorf tube, 170 μl reaction mixture consisting of 47 mM UDPGA, 25 mM $MgCl_2$, and 188 mM HEPES buffer (adjusted to pH 7.5) were mixed with 40 μl of enzyme source (liver S9 fraction or SF9 insect cell microsomes (UGT supersomes™) and 10 μl of substrate solution (100 mM of *1* in DMSO) giving a substrate concentration of 4.5 mM. The incubation was conducted at 37 °C and 950 rpm for 20 h with a closed vial top in a Thermomixer compact (Eppendorf, Hamburg, Germany) for the liver S9 incubations and for 4 h under the same conditions for the rh UGT-isoforms SF9 microsomal incubations. The reactions were stopped by adding 400 μl of a MeOH/ACN mixture (*v*/*v*; 1:1) and 10 min shaking at room temperature. After centrifugation, the supernatant was transferred to HPLC vials and analyzed by LC/MS-MS as described above. The following rh UGTs were tested for glucuronidation of 1: isoforms 1A1, 1A3, 1A4, 1A6, 1A7, 1A8, 1A9, 1A10, 2B4, 2B7, 2B10, 2B15, 2B17.

Preparative scale production and purification of glucuronide *3*

On a laboratory shaker (Adolf Kühner AG, Birsfelden, Switzerland), 56 ml of a solution of 32 mM ATP, 50 mM UDPGA, 25 mM $MgCl_2$, 250 mM HEPES buffer (adjusted to a pH of 7.5 with 5 N sodium hydroxide), and 40 mM NaCl was mixed with 14 ml of rat liver S9 preparation and 5 ml substrate solution (75 mM of 1 in DMSO) resulting in concentrations of 16.5 mg/ml protein and of 5 mM compound 1. The reaction was divided into 5 aliquots of 15–20 ml and incubated with closed cap in five 50 ml polyethylene tubes (Thermo Scientific 339652) at 37 °C and 230 rpm for 16 h utilizing a laboratory shaker. At the end of the incubation time, the reactions were frozen and stored until use at −20 °C.

After defrosting in a 50 °C water bath, the recombined reaction broth was mixed with two volume equivalents of an acetonitrile/methanol mixture (*v*/*v*; 1:1) and stirred at room temperature for 15 min. The broth was centrifuged at 8600*g* for 40 min, and the supernatant was filtrated through a paper filter. The filtrate was mixed with 675 ml of aqueous formic acid (0.05%) and pumped directly on the RP-18 chromatography column. The conditions for preparative HPLC were as follows: self-packed steel column 200 × 50 mm; stationary phase LiChroprep RP-18 40–63 μm (Merck KGaA, Darmstadt, Germany); mobile phase A, aqueous 0.05% formic acid; mobile phase B, methanol; gradient, 0–5 min 10% B, 48 min 95% B, 5 min 100% B; flow rate 5 ml/min; room temperature; detection at 220 nm; fraction size, 50 ml. The product eluted between 56 and 70% B. The product containing fractions were combined, and the solvents were partially removed under reduced pressure.

The remaining, now mainly aqueous solution, was mixed with 12 g of isolute absorbent (IST Ltd., Mid Glamorgan, UK) and with 25 ml of a mixture of methanol/dichloromethane (*v*/*v*; 20:80) and then evaporated to dryness in vacuo. The dry isolute coated with raw product was filled into a 50 × 25 mm pre-column. The second preparative HPLC was performed with a 250 × 21 mm Nucloeodur 100–10 C_{18} ec column (Macherey-Nagel, Düren, Germany) under the same conditions as described before. The product containing fractions were again combined, concentrated to about 50 ml and dried by lyophilization giving 50 mg of the product with an isolated yield of 30%. The purity was 96.8% of *3* and 3.2% of *2*.

Bioconversion on preparative scale and purification of glucuronide 2

The same procedure was followed for the preparation of *2* utilizing rabbit liver instead of rat liver S9 preparation. Purification of the glucuronide *2* was conducted in analogy to the one described above and yielded 55 mg of a mixture of 78% *2* and 22% of *3* corresponding to a yield of 33% for the mixture of the two glucuronides.

Results

A screening of 13 liver S9 homogenates from 11 vertebrate species was initiated under conditions suitable for glucuronidation utilizing UDPGA and investigated by LC-MS/MS. Under the initial LC conditions utilizing acetonitrile as an organic mobile phase and acidic conditions (0.02% trifluoroacetic acid in both mobile phases), a single peak for the two glucuronides was detected. It was, however, observed that the UV spectra in the DAD of some glucuronide samples were almost identical to the parent compound and some not. This prompted us to modify the LC conditions. By utilizing a pH of the mobile phase, where the glucuronic acid was deprotonated, several samples showed two, partially separated, peaks. A further improvement was achieved by replacing the organic mobile phase acetonitrile with methanol. The very high back pressure of a 15 cm long HPLC column filled with 1.7 μm particles and utilizing a viscous mobile phase like methanol was overcome by raising the column temperature to 45 °C and lowering the flow rate to 0.075 ml/min. A chromatogram is displayed in Additional file 1 with baseline separation of the two glucuronides and UV spectra of the three peaks. The earlier eluting peak of *2* had an UV spectrum very similar to the parent compound *1*, and for compound *3*, all absorption maxima were bathochromic shifted to higher wavelength. This different UV spectrum of *3* suggested—preliminary at this stage—that the chromophore was distorted presumably due to tautomerization of the 1*H*-indazole by attachment of the glucuronide at nitrogen-2.

The screening samples were quantified by LC-DAD close to the isobestic point of 240 nm that should give fairly accurate results for the conversions. The screening results (Table 1) showed that one species, rabbit, formed predominately the glucuronide *2*, several ones formed both in roughly equal amounts, and most animal species predominately glucuronide *3*, with guinea pig showing the highest selectivity. There was no correlation of the taxonomic order, as, for example, the species from the order Rodentia, mice, rat and guinea pig, had a very different specificity of their UDP-glucuronosyltransferases (UGTs). Experiments with compound *1* and human S9 liver fraction showed that predominately glucuronide *3* was formed and 19 times less of glucuronide *2* (Table 1).

Table 1 Percentage of glucuronide formation after exposure to liver species for 20 h (DAD at 240 nm) and selectivity for forming the glucuronide *3* sorted by increasing selectivity

Liver S9 homogenate from	*2*	*3*	Selectivity factor for *3* vs. *2*
Rabbit	30.5%	6.7%	0.2
Mice	6.0%	4.9%	0.8
Dog	2.9%	2.8%	1
Chicken	4.4%	9.6%	2
Mini pig (miniature pig)	1.4%	6.4%	5
Horse	<0.1%	0.7%	8 [a]
Foal	<0.1%	1.4%	8 [a]
Porcine	1.6%	12.7%	8
Bovine	1.8%	24.0%	10
Rat	1.4%	26.9%	20
Sheep	0.4%	17.2%	45
Cynomolgus monkey	0.2%	13.4%	55
Guinea pig	0.2%	21.5%	101
Human	4.1%	77.1%	19

[a]Data from MS trace

Considering that a preparative separation of the two closely eluting glucuronides by HPLC was impossible, the selection of the optimal animal species for large-scale preparation was essential. Rabbit liver was chosen as biocatalyst for the preparative production of glucuronide *2* and yielded 55 mg of a mixture of 78% *2* and 22% of *3* at a 100 mg scale. Rat liver was chosen to produce the glucuronide *3*, as the ratio of the glucuronides was similar to the one found after incubation with human liver S9 fraction. Preparative bioconversion with rat liver gave 50 mg of the desired product *3* with only 3.2% of *2*. The purity of the received material was sufficient to discriminate the two compounds in the NMR experiments necessary for structure elucidation. Structures *2* and *3* (Scheme 1) were identified as 1*N*- and 2*N*-glucuronides unambiguously based not only on the specific NOE correlations but also on distinctive differences in the observed chemical shifts as discussed in Additional file 1.

Among the 13 rh UGT-isoforms incubated with *1*, only UGT1A4 showed significant glucuronide formation of both glucuronides (see Table 2). The selectivity towards *N*-glucuronide *3* characterized by a selectivity factor of 33 was very similar to the one obtained with the human liver S9 preparation.

Discussion

The glucuronidation of 5-membered tertiary *N*-heterocycles are mainly mediated by UGT1A1 (pyrazoles, indazole in 1 position) (Berry et al. 2014; Smith et al. 2014), UGT1A3 (tetrazoles, pyrazoles) (Yan et al. 2006; Alonen et al. 2008), UGT1A9 (pyrazoles, triazoles) (Berry et al. 2014; Yan et al. 2006; Omura et al. 2007), UGT1A10 (tetrazoles, indazole in 1 position) (Alonen et al. 2008; Rose et al. 2009) or UGT2B7 (tetrazoles) (Alonen et al. 2008).On the other hand, N^+-glucuronides, like those of 1-imidazoles, are formed by UGT1A4 (Vashishtha et al. 2001). In the present study, we find that only rh UGT1A4 showed significant *N*-glucuronidation of *1*.

The formation of quaternary N^+-glucuronides from tertiary amines in aromatic *N*-heterocycles is one of the common reactions mediated by UGT1A4. In the case of the indazoles reported in this study, however, the nitrogen atom in the glucuronides is not a quaternary center. Glucuronides of this type have not been reported previously as products of UGT1A4. In addition, we find the energetically less favored glucuronide *3* as the main product formed by eight of the 11 animal species under investigation, including rat, by human liver S9 fraction as well as by rh UGT1A4 expressed in SF9 insect cells.

The 1*H*-tautomer of unsubstituted indazole is markedly more stable than the 2*H* form due to the lower aromaticity of the latter. With a Gibbs free energy of 15 $kJmol^{-1}$, the equilibrium constant is 51 in water (Minkin et al. 2000). For the two *N*-methyl-indazoles, this effect is even more pronounced and a theoretical equilibrium constant of 251 was calculated by Austin Model 1 semi-empirical quantum calculation (Öğretir and Tai 2002). As a consequence, the formation of the 2-glucuronide *3* required more energy in the enzymatic reaction than the one of the 1-glucuronide *2* (Scheme 1).

Mechanistically, two pathways can be envisaged for forming glucuronide *3*, either only the minor tautomer of *1* fits into the active site of UGT1A4 and therefore tautomerization takes place before the glucuronidation step and the energy required for the tautomerization originates from the binding energy to the enzyme or, more likely, the more stable tautomer of *1* is glucuronidated at nitrogen-2 by UGT1A4. The 1-*H* tautomer can either be glucuronidated in a concerted reaction or by forming a quaternary N^+-glucuronide that would react

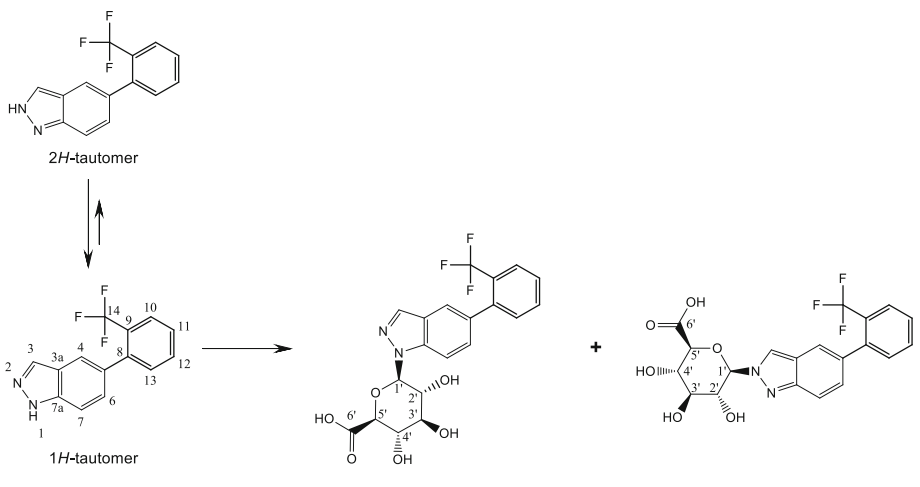

Scheme 1 Structures and atom numbering of drug candidate *1* and glucuronides *2* and *3*. Both tautomers of *1* are shown

Table 2 Percentage of glucuronide formation with recombinant human UDP-glucuronosyltransferases in supersomes™ after 4 h (DAD at 240 nm)

rh UDP-glucuronosyl-transferase	*2*	*3*	Selectivity factor for *3* vs. *2*
1A1	<0.2%	<0.2%	n.m.[a]
1A3	<0.2%	0.7%	>4
1A4	1.4%	47.4%	33
1A6	<0.2%	0.3%	>2
1A7	<0.2%	<0.2%	n.m.
1A8	<0.2%	<0.2%	n.m.
1A9	<0.2%	<0.2%	n.m.
1A10	<0.2%	<0.2%	n.m.
2B4	<0.2%	<0.2%	n.m.
2B7	<0.2%	<0.2%	n.m.
2B10	<0.2%	<0.2%	n.m.
2B15	<0.2%	<0.2%	n.m.
2B17	<0.2%	<0.2%	n.m.

[a]*n.m.* not meaningful

spontaneously to structure *3* with loss of a proton. As UGT1A4 is known to form many quaternary glucuronides (Kaivosaari et al. 2011), the second reaction mechanism seems more plausible and in line with reported data on UGT1A4. Thus, the reaction may well proceed via the expected formation of quaternary N^+-glucuronide from tertiary amines, but due to the higher stability of the deprotonated tautomer, products are obtained, which have not been previously reported for UGT1A4 both in terms of regioselectivity and absence of quaternization of the nitrogen.

For example, the structure of axitinib, an inhibitor of vascular endothelial growth factor receptors tyrosine kinase, contains a disubstituted 1H-indazole moiety (Smith et al. 2014). In human studies with [^{14}C]axitinib, *N*-glucuronidation occurred at the more stable nitrogen-1 of the indazole moiety and the reaction was primarily catalyzed by UGT1A1, which is contrary to our findings with compound *1*, where the less stable tautomer was the attachment point of the human glucuronide and UGT1A4 the active human isoform.

The MS/MS spectra of both glucuronides (Fig. 1, Additional file 1) were dominated by *m/z* 263 corresponding to the loss of glucuronic acid which is typical for glucuronides (Stachulski and Meng 2013) and the loss of one or two water molecules. The spectra showed, however, subtle differences. The fragments *m/z* 421 (loss of one water molecule) and *m/z* 305 (loss of 134 Da) were noticeably larger in the spectrum of 1-glucuronide *2*.

The loss of 134 Da or $C_4H_6O_5$ as a major fragment from glucuronides is quite rare and raises two questions: Under which conditions is this fragment formed, or in other words, why was it observed with compound *2* and not by *1* and, secondly, what is the fragmentation mechanism. This neutral loss has been described mainly for *N*-glucuronides (Amore et al. 1997; Erve et al. 2007; Kassahun et al. 1997), a thiocarbamate *N*-glucuronide

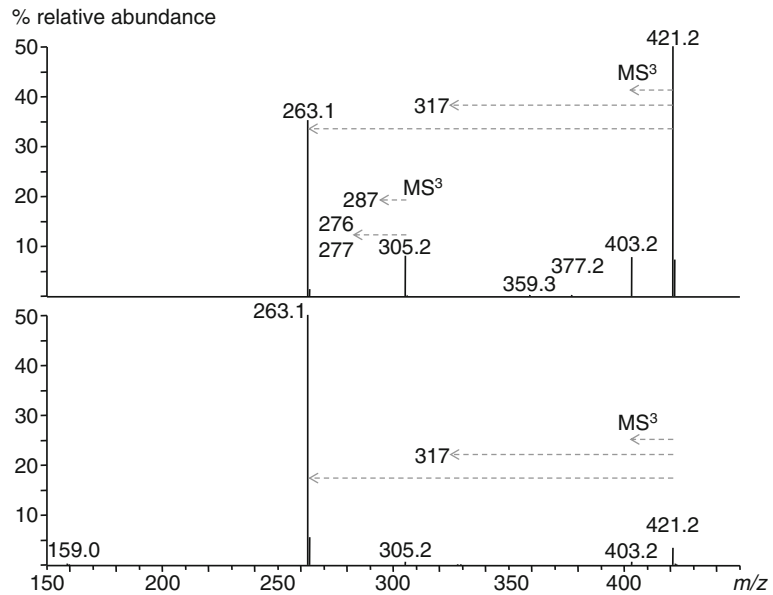

Fig. 1 CID product ion spectra of *m/z* 439.1 of glucuronides *2* (upper spectrum) and *3* (lower spectrum) magnified by a factor of two. Important MS^3 fragments are indicated by *dashed arrows*

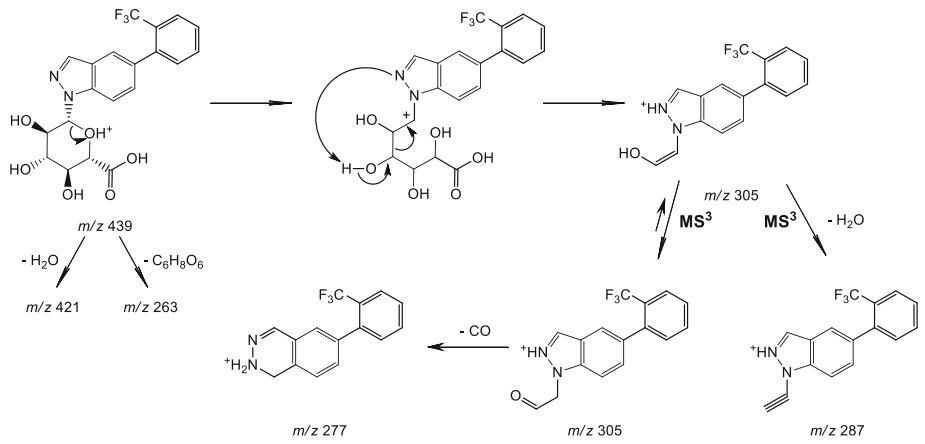

Scheme 2 Proposed MS/MS fragmentation mechanism of glucuronide *2*

originating from pioglitazone (Uchiyama et al. 2010) and recently also for a glucuronide of GTx-024 ((S)-*N*-(4-cyano-3-(trifluoromethyl)phenyl)-3-(4-cyanophenoxy)-2-hydroxy-2-methylpropanamide) for that an *O*-glucuronide was proposed (Kim et al. 2013). Olanzapine formed two *N*-glucuronides, one at the secondary nitrogen-10 and one at the tertiary nitrogen-4′ with distinctly different MS/MS spectra (Kassahun et al. 1997). The fragment *m/z* 355 (loss of 134 Da) had a relative intensity of 70% for the 10-*N*-glucuronide and was very small for the 4′-N^+-glucuronide. This suggested that one of the deciding factors for the formation of this neutral loss of 134 Da was the site of the positive charge, whereby a charge directly at the glucuronide-binding nitrogen inhibited this fragmentation pathway. The same was true for glucuronides *2* and *3*: Glucuronide *2* was more likely protonated at attaching nitrogen as the proton affinity (PA) of 2*N*-methyl-indazole (905 $kJmol^{-1}$) was markedly larger than that of 1*N*-methyl-indazole (875 $kJmol^{-1}$) (Öğretir and Kaipak 2002). Glucuronide *3*, in turn, was more likely protonated at different locations including at the glucuronic acid moiety. Both PA values were large enough for ionization with ESI, where a PA larger than 854 $kJmol^{-1}$ seemed necessary (Kostiainen and Kauppila 2009). In conclusion, the MS^2 fragmentation pattern of olanzapine glucuronides and the proton affinity of model compounds could explain that in *3*, the N-2 was protonated and that therefore almost no loss of 134 Da was observed. Other examples, where the site of the protonation influenced the MS/MS fragmentation pattern, have been described (Kaufmann et al. 2009; Wang et al. 2010).

A mechanism for the formation of *m/z* 305 is proposed in Scheme 2. The fragmentation reaction started from the parent molecule without previous loss of water, as neither *m/z* 421 $[M - H_2O + H]^+$ nor *m/z* 403 $[M-2 H_2O + H]^+$ fragmented further to *m/z* 305 in MS^3 experiments. The oxygen in the fragment *m/z* 305 should to be in 2′ position, as loss of carbon monoxide (−28 Da) was observed in the MS^3 spectrum of *m/z* 305. The proposed mechanism was consistent with HR-MS and MS^3 experiments.

Conclusions

This investigation shows that assumptions on the structure of metabolites based on stability of tautomers may be wrong. For substituted indazoles and related compounds, a purification of such a metabolite to perform structure elucidation should not be necessary as already the information gained from the UV spectrum by a DAD detector should be sufficient to assign a tentative structure. In conclusion, two *N*-glucuronides were isolated from a substituted 1H-indazole and their structure as well as some physicochemical parameters determined. A novel mechanism to form tertiary *N*-glucuronides was proposed. Possibly, the UPLC parameters to achieve baseline separation of the two glucuronides can be applied to other cases of difficult to separate glucuronides.

Additional files

Additional file 1: Structure elucidation of compounds *2* and *3*. ^{13}C-, ^{15}N-, and ^{1}H-NMR assignments and HMBC correlations for *1* to *3*. Accurate mass data of glucuronides *2* and *3* and elemental composition of MS/MS fragments. HPLC chromatogram of rabbit liver screening and UV spectra. Origin of animals and protein concentrations. (DOC 160 kb)

Acknowledgements

We thank Dr. Christian Guenat for the HR-MS measurement, Alexandra Vargas for the preparation of the liver S9-fractions, and Dr. Eric Francotte and PD Dr. Stephan Lütz for the continuous support of this work. Thanks are also due to Dr. Lisa Rooney, Novartis Horsham, UK, for providing the compound.

Authors' contributions

AF, FKE, and JK conducted the experiment. AF, MK, and TL performed the data analysis. AF, FKE, MK, and TL contributed to the writing. All authors read and approved the final manuscript.

Competing interests
The authors declare that they have no competing interests.

Publisher's Note

Received: 25 January 2017 Accepted: 11 April 2017
Published online: 29 April 2017

References

Alonen A, Finel M, Kostiainen R. The human UDP-glucuronosyltransferase UGT1A3 is highly selective towards N2 in the tetrazole ring of losartan, candesartan, and zolarsartan. Biochem Pharmacol. 2008;76:763–72.

Amore BM, Kalhorn TF, Skiles GL, Hunter AP, Bennett GD, Finnell RH, Nelson SD, Slattery JT. Characterization of carbamazepine metabolism in a mouse model of carbamazepine teratogenicity. Drug Metab Dispos. 1997;25:953–62.

Berry LM, Liu J, Colletti A, Krolikowski P, Zhao Z, Teffera Y. Species difference in glucuronidation formation kinetics with a selective mTOR inhibitor. Drug Metab Dispos. 2014;42:707–17.

Chen J, McGaraughty S, Kym PR. TRPA1 in drug discovery. In: Szallasi A, Biro T, editors. TRP channels in drug discovery, vol. 1. Heidelberg: Springer/Humana Press; 2012. p. 43–59.

Erve JCL, Vashishtha SC, DeMaio W, Talaat RE. Metabolism of prazosin in rat, dog, and human liver microsomes and cryopreserved rat and human hepatocytes and characterization of metabolites by liquid chromatography/tandem mass spectrometry. Drug Metab Dispos. 2007;35:908–16.

Kaivosaari S, Finel M, Koskinen M. *N*-glucuronidation of drugs and other xenobiotics by human and animal UDP-glucuronosyltransferases. Xenobiotica. 2011;41:652–69.

Kassahun K, Mattiuz E, Nyhart Jr E, Obermeyer B, Gillespie T, Murphy A, Goodwin AR, Tupper D, Callaghan JT, Lemberger L. Disposition and biotransformation of the antipsychotic agent olanzapine in humans. Drug Metab Dispos. 1997; 25:81–93.

Kaufmann A, Butcher P, Maden K, Widmer M, Giles K, Uría D. Are liquid chromatography/electrospray tandem quadrupole fragmentation ratios unequivocal confirmation criteria? Rapid Commun Mass Spectrom. 2009;23: 985–98.

Kim J, Wang R, Veverka KA, Dalton JT. Absorption, distribution, metabolism and excretion of the novel SARM GTx-024 [(S)-*N*-(4-cyano-3-(trifluoromethyl)phenyl)-3-(4-cyanophenoxy)-2-hydroxy-2-methylpropanamide] in rats. Xenobiotica. 2013;43:993–1009.

Kittelmann M, Rheinegger U, Espigat A, Oberer L, Aichholz R, Francotte E, Ghisalba O. Preparative enzymatic synthesis of the acylglucuronide of mycophenolic acid. Adv Synth Catal. 2003;345:825–9.

Koivisto A, Chapman H, Jalava N, Korjamo T, Saarnilehto M, Lindstedt K, Pertovaara A. TRPA1: a transducer and amplifier of pain and inflammation. Basic Clin Pharmacol Toxicol. 2014;114:50–5.

Kostiainen R, Kauppila TJ. Effect of eluent on the ionization process in liquid chromatography-mass spectrometry. J Chromatogr A. 2009;1216:685–99.

Kremeyer B, Lopera F, Cox JJ, Momin A, Rugiero F, Marsh S, Woods CG, Jones NG, Paterson KJ, Fricker FR, Villegas A, Acosta N, Pineda-Trujillo NG, Ramírez JD, Zea J, Burley MW, Bedoya G, Bennett DLH, Wood JN, Ruiz-Linares A. A gain-of-function mutation in TRPA1 causes familial episodic pain syndrome. Neuron. 2010;66:671–80.

Minkin VI, Garnovskii AD, Elguero J, Katritzky AR, Denisko OV. The tautomerism of heterocycles: five-membered rings with two or more heteroatoms. Adv Heterocycl Chem. 2000;76:157–323.

Moran MM, McAlexander MA, Biro T, Szallasi A. Transient receptor potential channels as therapeutic targets. Nat Rev Drug Discov. 2011;10:601–20.

Öğretir C, Kaipak NF. Quantum chemical calculations on the annular tautomerism of some indazole derivatives. 1. A gas phase study. J Mol Struct (THEOCHEM). 2002;583:137–44.

Öğretir C, Tai NF. Investigation of the structure and properties of some indazole derivatives using the AM1, PM3 and MNDO semiempirical methods. 2. An aqueous phase study. J Mol Struct (THEOCHEM). 2002;588:145–53.

Omura K, Nakazawa T, Sato T, Iwanaga T, Nagata O. Characterization of N-glucuronidation of 4-(5-pyridin-4-yl-1H-[1,2,4]triazol-3-yl)pyridine-2-carbonitrile (FYX-051): a new xanthine oxidoreductase inhibitor. Drug Metab Dispos. 2007;35:2143–8.

Rooney L, Vidal A, D'Souza A-M, Devereux N, Masick B, Boissel V, West R, Head V, Stringer R, Lao J, Petrus M, Patapoutian A, Nash M, Stoakley N, Panesar M, Verkuyl JM, Schumacher AM, Petrassi HM, Tully DC. Discovery, optimization, and biological evaluation of 5-(2-(trifluoromethyl)phenyl)-indazoles as a novel class of transient receptor potential A1 (TRPA1) antagonists. J Med Chem. 2014;57:5129–40.

Rose K, Yang YS, Sciotti R, Cai H. Structure-activity relationship (SAR): effort towards blocking *N*-glucuronidation of indazoles (PF-03376056) by human UGT1A enzymes. Drug Metab Lett. 2009;3:28–34.

Smith BJ, Pithavala Y, Bu H-Z, Kang P, Hee B, Deese AJ, Pool WF, Klamerus KJ, Wu EY, Dalvie DK. Pharmacokinetics, metabolism, and excretion of [^{14}C]axitinib, a vascular endothelial growth factor receptor tyrosine kinase inhibitor, in humans. Drug Metab Dispos. 2014;42:918–31.

Stachulski AV, Meng X. Glucuronides from metabolites to medicines: a survey of the *in vivo* generation, chemical synthesis and properties. Nat Prod Rep. 2013;30:806–48.

Uchiyama M, Fischer T, Mueller J, Oguchi M, Yamamura N, Koda H, Iwabuchi H, Izumi T. Identification of novel metabolic pathways of pioglitazone in hepatocytes: *N*-glucuronidation of thiazolidinedione ring and sequential ring-opening pathway. Drug Metab Dispos. 2010;38:946–56.

Vashishtha SC, Hawes EM, McKay G, McCann DJ. Quaternary ammonium-linked glucuronidation of 1-substituted imidazoles: studies of human UDP-glucuronosyltransferases involved and substrate specificities. Drug Metab Dispos. 2001;29:1290–5.

Wang J, Aubry A, Bolgar MS, Gu H, Olah TV, Arnold M, Jemal M. Effect of mobile phase pH, aqueous-organic ratio, and buffer concentration on electrospray ionization tandem mass spectrometric fragmentation patterns: implications in liquid chromatography/tandem mass spectrometric bioanalysis. Rapid Commun Mass Spectrom. 2010;24:3221–9.

Wu LJ, Sweet TB, Clapham DE. International union of basic and clinical pharmacology. LXXVI. Current progress in the mammalian TRP ion channel family. Pharmacol Rev. 2010;62:381–404.

Yan Z, Caldwell GW, Gauthier D, Leo GC, Mei J, Ho CY, Jones WJ, Masucci JA, Tuman RW, Galemmo Jr RA, Johnson DL. *N*-glucuronidation of the platelet-derived growth factor receptor tyrosine kinase inhibitor 6,7-(dimethoxy-2,4-dihydroindeno[1,2-c]pyrazol-3-yl)-(3-fluorophenyl)-amine by human UDP-glucuronosyltransferases. Drug Metab Dispos. 2006;34:748–55.